Noise-Adjusted Principal Component Analysis for Buried Radioactive Target Detection and Classification

Qian Du, *Senior Member, IEEE*, Wei Wei, *Student Member, IEEE*, Daniel May, *Member, IEEE*, and Nicolas H. Younan, *Senior Member, IEEE*

***Abstract*—We present a noise-adjusted principal component analysis (NAPCA)-based approach to the detection and classification of buried radioactive targets with short sensor dwell time. The data used in the experiments is the gamma spectroscopy collected by a Sodium Iodide (NAI) scintillation detector. Spectral transformation methods are first applied to the data, followed by NAPCA. Then k-nearest neighbor (kNN) clustering is applied to the NAPCA-transformed feature subspace to achieve detection or classification. This method is evaluated using a database of 240 spectral measurements consisting of background (construction sand), benign material measurements (uranium ore), and target measurements (depleted uranium) at various depths. Compared to other widely used algorithms for depleted uranium, the proposed technique can provide better performance.**

***Index Terms*—Buried target detection, classification, Gamma-ray spectral analysis, noise-adjusted principal component analysis, principal component analysis.**

I. Introduction

THE detection and discrimination of radioactive objects has many important applications, such as illicit cargo detection at border crossings [1], [2], buried target detection within battlefields [3], and nuclear threat discrimination from benign sources [4]. Several approaches have been developed [4]–[6]. Many of these methods use a gamma spectrometer to count the number of emitted gamma photons and detection or classification is achieved based on the measurements of these photons at different energy levels. It is assumed that the collected energy spectrum is significantly different between target and non-target measurements. For instance, one of the most common and simple criteria is the gross count (GC) of photons within different spectral energy channels [4]. Another method involves computing the ratio of an unknown measurement with a known and benign measurement, which is referred to as the spectral comparison ratio (SCR) method [4], [5]. Characteristics of the ratio can help determine whether the unknown measurement is similar to that of benign measurement; then target discrimination can be achieved.

Due to low energy counts and strong background clutters, the performance of the aforementioned techniques may be poor when a target, e.g., depleted uranium, is buried. The problem becomes more challenging if the sensor dwell time (i.e., counting period) is very short, e.g., 1 s. Under such circumstance, it is important to develop algorithms that can effectively suppress noise and background interference. In this paper, we will investigate three spectral transformation methods, including spectral bin energy (SBE), spectral bin ratio (SBR), and SCR, which can normalize the contribution from background and eliminate the trivial variation from noise.

Principal component analysis (PCA) has the capability of suppressing noise as well. PCA can compact data information into major principal components (PCs) since it ranks PCs in terms of data variance. The rationale of applying PCA is that noise effect can be alleviated if only major PCs participate in the following data analysis. It assumes that important signal features are included in major PCs. PCA has been applied to gamma-ray spectra for anomaly detection [7]. In this paper, we apply PCA to the detection and classification of buried targets. The PCs holding the highest levels of variance are considered as features of the spectra. From these features, each spectrum is classified using k-nearest neighbor (kNN) clustering [8]. If clustering is conducted for two classes, i.e., target class and non-target class, then detection can be achieved. In addition, the three aforementioned spectral transformation methods are employed before PCA. Experimental results show that this method, i.e., spectral transformation followed by PCA, may provide better performance than applying transformation only.

However, it is obvious that both signal and noise can contribute to data variance; it is possible for a PC with lower ranking to include more important signal features than a PC with higher ranking. Thus, noise-adjusted principal component analysis (NAPCA) was proposed, which is to rank PCs in terms of signal-to-noise ratio (SNR) [9], [10]. SNR is a better metric than variance to gauge the actual signal information contained in major PCs. In this way, a PC with higher ranking always contains more signal information and less noise than a PC with lower ranking. The idea of NAPCA was originally proposed for image processing. In this paper, we will deploy NAPCA for the analysis of gamma-ray data. The experimental result demonstrates that NAPCA is better than PCA in extracting data

Manuscript received December 31, 2009; revised May 17, 2010, June 14, 2010, September 18, 2010; accepted September 27, 2010. Date of current version December 15, 2010. This work was supported by the U.S. Army Engineer Research and Development Center at Vicksburg, Mississippi.

The authors are with the Department of Electrical and Computer Engineering, Mississippi State University, Mississippi State, MS 39762 USA (e-mail: du@ece.msstate.edu).

Color versions of one or more of the figures in this paper are available online at http://ieeexplore.ieee.org.

Digital Object Identifier 10.1109/TNS.2010.2084105

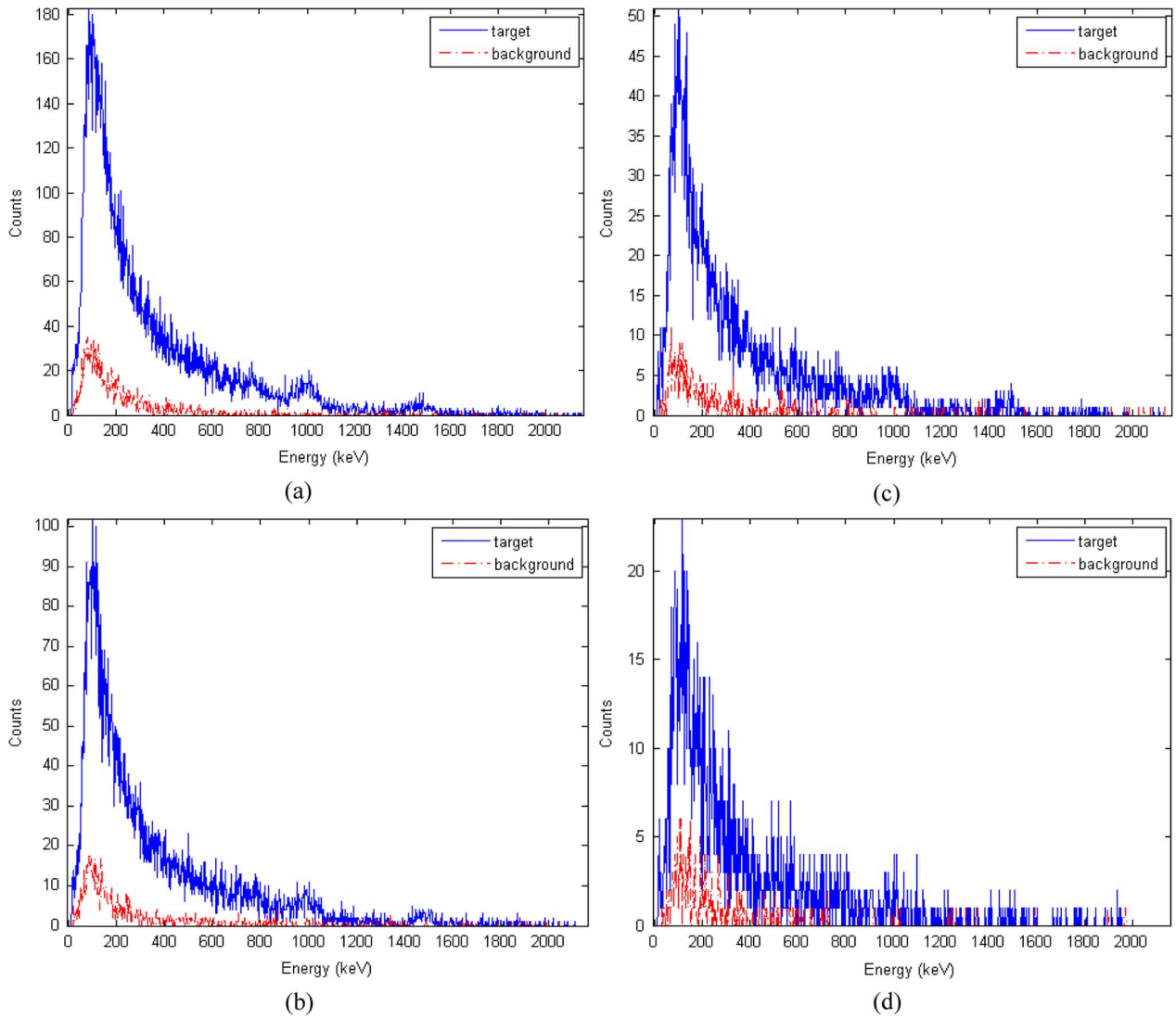

Fig. 1. Energy spectra with different sensor dwell time. (a). Original target (DU buried 15 cm deep) and background spectra (dwell time is 1 s), (b). Original target (DU buried 15 cm deep) and background spectra (dwell time is 0.5 s), (c). Original target (DU buried 15 cm deep) and background spectra (dwell time is 0.25 s), (d). Original target (DU buried 15 cm deep) and background spectra (dwell time is 0.1 s).

features, thereby achieving higher detection and classification accuracy.

It is noteworthy that the computation of data covariance matrix and its eigen-decomposition are the major steps when implementing PCA and NAPCA. To make the covariance matrix full-rank, the number of independent samples should be greater than the number of data dimensionality, which is the number of spectral channels. Thus, the three spectral transformation methods, i.e., SBE, SBR, and SCR, can help to alleviate the requirement for a large number of independent spectral measurements via data dimensionality reduction.

II. Spectral Transforms

Each measurement contains some degree of variability and uncertainty in the number of counts detected. It may be difficult to compare two measurements taken over during different time periods. Fig. 1 shows the energy spectra collected by 1 s, 0.5 s, 0.25 s, and 0.1 s. With the dwell time being reduced, the spectrum becomes sparser. Thus, it may be helpful to map each spectrum into a certain range by normalizing the count in each energy channel according to the total amount of counts within the spectral coverage. As shown in (1), $P(l)$ and $\hat{P}(l)$ are energy counts at the lth channel before and after normalization, and L is the total number of channels

$$\hat{P}(l) = \frac{P(l)}{\sum_{l=0}^{L-1} P(l)}. \tag{1}$$

Then the following data processing uses the transformed $\hat{P}(l)$.

A. Spectral Bin Energy (SBE)

The input spectral measurements are divided into fixed-width, overlapping bins with width m and step-size s. The sum of energy within each bin is computed as

$$S_{\mathrm{SBE}}(j) = \sum_{i=js}^{js+m-1} \hat{P}(i) \quad \text{for} \quad j = 0, 1, \ldots, J-1 \tag{2}$$

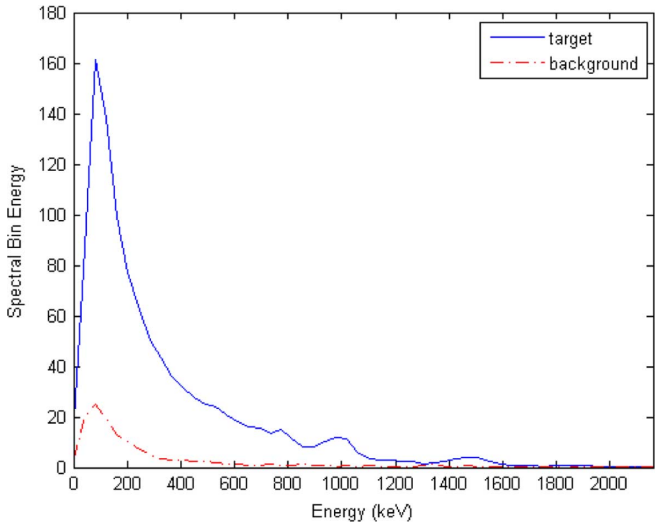

Fig. 2. SBE curves of the background and target spectra in Fig. 1(a).

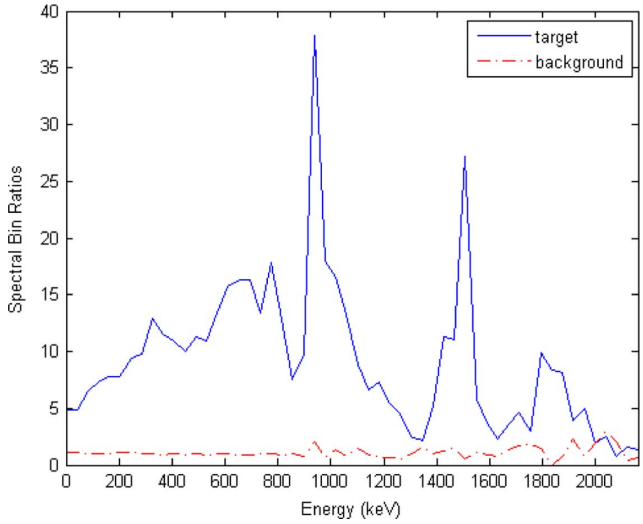

Fig. 3. SBRs of the background and target spectra in Fig. 1(a).

where J is the total number of bins after transformation, thus reducing the size of the set of values that describes the spectrum. For spectrum measurements that are significantly sparse, such as those measured with short sensor dwell time, this transform is especially useful since it helps summarize information within the spectrum that might not be immediately obvious and eliminate nuisance variations of the spectrum that do not contribute useful information. As mentioned earlier, it also reduces the data dimensionality (from the number of energy channels to the number of energy bins), which reduces the number of samples required to estimate a data covariance matrix with full rank in the following PCA or NAPCA.

Note that (2) is a general expression for any m and s with overlapping bins. Due to the difficulty of determining the optimal parameters, we simply use evenly spaced non-overlapping bins in the experiment with $m = s$. Then the optimal bin-width m can be found by exhaustive searching. In this research, the m is simply selected such that each bin has non-zero counts; the other two ratio-based transforms, i.e., SBR and SCR, are built upon SBE, so this choice makes them feasible. Fig. 1 illustrates original spectra from 0 keV to 2160 keV with 1011 spectral channels before the SBE transform, and the SBE-transformed spectra for those in Fig. 1(a) with $m = 40$ keV are illustrated in Fig. 2, where the major spectral features are still visible but with much less random variation.

B. Spectral Bin Ratios (SBR)

The second method transforms the spectrum based on its ratio with a previously measured background spectrum. The spectrum is divided into several bins. The sum of the energy within each bin is computed for both the observed spectrum and the known background spectrum, and the ratio of these two sums is computed using (3). For the jth bin

$$S_{\mathrm{SBR}}(j) = \frac{S_{\mathrm{SBE}}(j)}{S^b_{\mathrm{SBE}}(j)} \quad \text{for} \quad j = 0, 1, \ldots, J-1 \tag{3}$$

where S^b_{SBE} and S_{SBE} are the SBE-transformed known background and observed measurements, respectively. Fig. 3 illustrates a comparison of the ratios of the background measurement and the target measurement in Fig. 1(a) using another background measurement in (3). Notice that the background ratio is close to 1 across the spectrum. This is expected since all background measurements should have a similar fraction of energy for each energy channel. On the other hand, the ratio for target measurement is dramatically different and easily distinguishable from the background ratio.

C. Spectral Comparison Ratios (SCR)

The third method uses the SCR [5], [6]. As with the SBR method, a previously measured background spectrum is required. Both the known background spectrum and the observed spectrum are divided into fixed-width, non-overlapping bins as in SBE. One bin (usually the first bin) is chosen as a reference. The SCR can then be computed as:

$$S_{\mathrm{SCR}}(j) = S_{\mathrm{SBE}}(0) - \frac{S^b_{\mathrm{SBE}}(0)}{S^b_{\mathrm{SBE}}(j)} S_{\mathrm{SBE}}(j) \quad \text{for} \quad j = 0, 1, \ldots, J-1. \tag{4}$$

Given an observed spectral measurement, SCR measures how closely the spectrum matches that of the background. If the observed spectrum is a background measurement, the SCR is close to 0 across the spectrum; otherwise, the magnitude of the SCR should be significantly higher than 0. Fig. 4 shows the SCR-transformed spectra for the two spectra in Fig. 1(a), whose difference is significant. Actually, this difference is magnified compared to the original spectra.

III. PCA and NAPCA-based Approaches

A. PCA and NAPCA

PCA ranks PCs in terms of data variance. Consider the observation model

$$\mathbf{r} = \mathbf{x} + \mathbf{n} \tag{5}$$

where $\mathbf{r}$ is an energy spectral measurement with data dimensionality L (i.e., the number of spectral channels), $\mathbf{x}$ is a signal

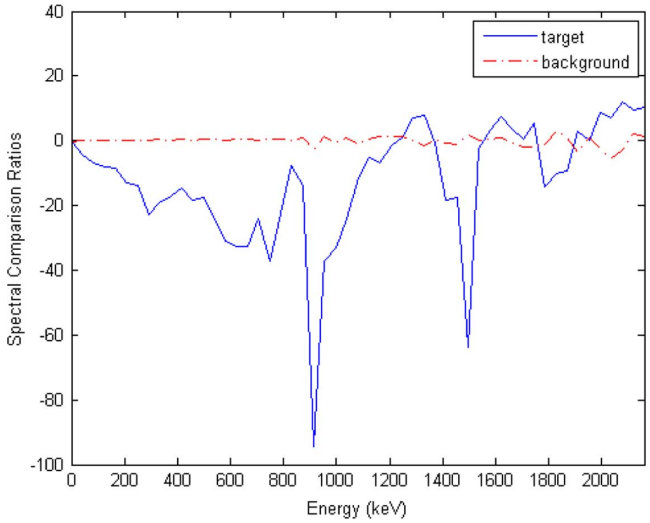

Fig. 4. SCRs of the background and target spectra in Fig. 1(a).

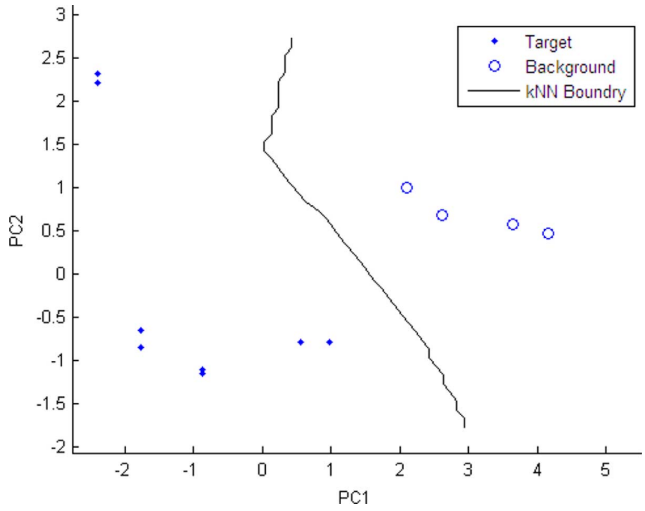

Fig. 5. Decision boundary determined by training data.

vector, and $\mathbf{n}$ represents the uncorrelated additive noise. Let $\mathbf{V} = [\mathbf{v}_1, \mathbf{v}_2, \ldots, \mathbf{v}_L]$ and $\mathbf{\Lambda} = \text{diag}\{\lambda_1, \lambda_2, \ldots, \lambda_L\}$ be the eigenvector and eigenvalue matrices of the data covariance matrix $\mathbf{\Sigma}$, where $\mathbf{v}_1, \mathbf{v}_2, \ldots, \mathbf{v}_L$ are L eigenvectors of size $L \times 1$ and $\lambda_1, \lambda_2, \ldots, \lambda_L$ are the corresponding L eigenvalues, i.e.,

$$\mathbf{V}^T \mathbf{\Sigma} \mathbf{V} = \mathbf{\Lambda}. \tag{6}$$

Then, the PC images can be calculated from

$$\mathbf{r}_{\text{PCA}} = \mathbf{\Lambda}^{-1/2} \mathbf{V}^T (\mathbf{r} - \mathbf{m}) \tag{7}$$

where $\mathbf{m}$ is the data mean. Assume $\lambda_1 \geq \lambda_2 \geq, \ldots, \geq \lambda_L$, the variances of the L PC images of the transformed data using $\mathbf{r}_{\text{PCA}}$ are $\lambda_1, \lambda_2, \ldots, \lambda_L$, respectively.

NAPCA ranks PCs in terms of SNR. It can be performed with two steps. The first step conducts noise-whitening to the original data, and the second step performs the ordinary PCA to the noise-whitened data. Since the noise variance is unity in the noise-whitened data, the resultant PCs are in the order of SNR. Let $\mathbf{\Sigma}_n$ be the noise covariance matrix and $\mathbf{F}$ be the noise-whitening matrix such that

$$\mathbf{F}^T \mathbf{\Sigma}_n \mathbf{F} = \mathbf{I} \tag{8}$$

where $\mathbf{I}$ is the identity matrix. Transforming $\mathbf{\Sigma}$ by $\mathbf{F}$, i.e.,

$$\mathbf{F}^T \mathbf{\Sigma} \mathbf{F} = \mathbf{\Sigma}_{n\_\text{adj}} \tag{9}$$

where $\mathbf{\Sigma}_{n\_\text{adj}}$ is the covariance matrix with the noise being whitened. Finding a matrix $\mathbf{G}$ such that

$$\mathbf{G}^T \mathbf{\Sigma}_{n\_\text{adj}} \mathbf{G} = \mathbf{I}. \tag{10}$$

Then, the operator for NAPCA can be constructed by

$$\mathbf{r}_{\text{NAPCA}} = \mathbf{G}^T \mathbf{F}^T (\mathbf{r} - \mathbf{m}). \tag{11}$$

The major difficulty in performing NAPCA is having an accurate noise covariance matrix $\mathbf{\Sigma}_n$. The following method is adopted in our research for its simplicity and effectiveness [11]. Let $\mathbf{\Sigma}$ be decomposed as

$$\mathbf{\Sigma} = \mathbf{DED} \tag{12}$$

where $\mathbf{D} = \text{diag}\{\sigma_1, \sigma_2, \ldots, \sigma_L\}$ is a diagonal matrix with σ_l^2 being the diagonal elements of $\mathbf{\Sigma}$, which is the variance of the lth original channel, and $\mathbf{E}$ is the correlation coefficient matrix whose ijth element represents the correlation coefficient between the ith and jth channels. Similarly, in analogy with the decomposition of $\mathbf{\Sigma}$, its inverse $\mathbf{\Sigma}^{-1}$ can be also decomposed as

$$\mathbf{\Sigma}^{-1} = \mathbf{D}_{\mathbf{\Sigma}^{-1}} \mathbf{E}_{\mathbf{\Sigma}^{-1}} \mathbf{D}_{\mathbf{\Sigma}^{-1}} \tag{13}$$

where $\mathbf{D}_{\mathbf{\Sigma}^{-1}} = \text{diag}\{\zeta_1, \zeta_2, \ldots, \zeta_L\}$ is a diagonal matrix with ζ_l^2 being the diagonal elements of $\mathbf{\Sigma}^{-1}$ and $\mathbf{E}_{\mathbf{\Sigma}^{-1}}$ is a matrix similar to $\mathbf{E}$ with the diagonal elements being one and all the off-diagonal elements being within $(-1, 1)$. It turns out that ζ_l^2 is the reciprocal of a good noise variance estimate of the lth channel. Therefore, the noise covariance matrix $\mathbf{\Sigma}_n$ can be estimated by a diagonal matrix $\mathbf{\Sigma}_n = \text{diag}\{\zeta_1^{-2}, \zeta_2^{-2}, \ldots, \zeta_L^{-2}\}$.

It is worth mentioning that data dimensionality may be reduced to J if energy bins are applied in spectral transformation.

B. Target Detection and Evaluation

To extract the primary features from data contaminated by noise and background clutter, PCA or NAPCA can be applied to the transformed spectra. The first several PCs are kept and used in the detection or classification step. The kNN clustering technique is applied to the PCs. For detection, the reduced set of features can be classified into two classes, e.g., target and non-target (or background), using the kNN. Fig. 5 illustrates an example that shows the decision boundary created by the kNN method. In this case, there are a total of four background measurements and eight target measurements. The decision boundary consists of the points whose average distances to the k nearest target samples and to the k nearest background samples are the same. We choose k to be 2 in this example. All the test measurements to one side of the decision boundary will be

detected as the background, and all measurements to the other side will be detected as the target. Similarly, multiple-class classification is achieved with multiple boundaries.

Detection performance is quantified with target detection (TD) accuracy, non-target detection (NTD) accuracy, and overall detection (OD) accuracy. In addition, targets buried at different depth can be considered as different classes, and classification accuracy can be quantified using target classification (TC) accuracy and overall classification (OC) accuracy. Specifically, the five metrics are defined as

$$\begin{aligned}
\mathrm{TD} &= \frac{\text{number of accurately detected target samples}}{\text{number of target samples}} \\
\mathrm{NTD} &= \frac{\text{number of accurately detected nontarget samples}}{\text{number of nontarget samples}} \\
\mathrm{OD} &= \frac{\text{number of accurately detected samples}}{\text{number of overall samples}}. \\
\mathrm{TC} &= \frac{\text{number of accurately classified target samples}}{\text{number of target samples}} \\
\mathrm{OC} &= \frac{\text{number of accurately classified samples}}{\text{number of overall samples}}. \qquad (14)
\end{aligned}$$

IV. Experiments

Laboratory data were taken using a $10 \times 10 \times 40$ cm sodium iodide (NaI) scintillation detector. ORTEC DigiBASE with ORTEC GammaVision software was employed. The measured spectra cover the energy range of 0 keV to 2160.0 keV. After SBE, SBR, and SCR, each measurement had 54 bins ($m = 40$ keV). Note that this bin-width was not optimized. The target was a cylindrical object with 4.3 kg mass. The background conditions consisted of construction sand, and small-rock-type uranium ore was considered a benign object.

The target was buried at 15 cm, 23 cm, 30 cm, 45 cm, 60 cm, 75 cm, and 90 cm depth. Natural ore in a quart-size plastic bag was buried at 45 cm and 75 cm depth. Each class had 24 samples. Sensor dwell time was varied from 1 s, 0.5 s, 0.25 s, to 0.1 s. Before processing, all the measurements were normalized into equivalent 1 s dwell time. Training samples were needed for each class (including background) at different depths. The final performance may be slightly changed with the number of PCs used, and we found out that using the first two PCs could provide the best overall performance in our experiments. Thus, we presented the results using the first two PCs hereafter.

A. Experiment Using the Entire Dataset

kNN ($k = 4$) was applied for T-fold cross-validation ($T = 24$). The T-fold cross-validation divided the original samples into T subsamples. Of the T subsamples, a single subsample was taken for validation and the remaining $T - 1$ subsamples were used as training data. The cross-validation process was then repeated T times, with each of the T subsamples used exactly once as the validation data. The T results from the folds were averaged to produce a single estimation. All samples were used for both training and validation, and each sample was used for validation exactly once.

TABLE I
Detection and Classification Accuracy (%) of Different Methods for the Entire Dataset

Methods	TD	NTD	OD	TC	OC
GC	83.7	63.5	77.6	80.3	63.8
SBE	91.6	83.3	89.1	81.8	75.5
SBR	90.5	40.3	75.4	69.0	54.6
SCR	89.3	69.4	83.3	77.4	70.4
SBE-PCA	93.5	88.9	92.1	72.6	71.3
SBR-PCA	73.8	62.5	70.4	48.8	41.7
SCR-PCA	89.3	73.6	84.6	64.9	61.7
SBE-NAPCA	94.3	88.3	92.5	87.1	77.0
SBR-NAPCA	93.9	87.3	91.9	87.1	76.7
SCR-NAPCA	93.2	77.8	88.6	81.6	75.7

Table I tabulates the average detection accuracy of cross-validation by considering all the seven target classes as a single class and all the three non-target classes as the other. The NAPCA-based methods provided higher detection accuracy than the PCA-based methods. In particular, the three spectral transformation methods in conjunction with NAPCA could improve the performance of the methods applied on the original data. For instance, the SBR transform could not improve the performance if using PCA; however, it could result in significant improvement with NAPCA. As for the SCR method, the overall detection (OD) accuracy was lower than the NAPCA-based method, but similar to the PCA-based method; with PCA (i.e., SCR-PCA), the OD accuracy was slightly increased from 83.3% to 84.6%; if NAPCA was employed (i.e., SCR-NAPCA), it was further increased to 88.6%. The GC method generally yielded low accuracy.

Classification was also conducted where targets buried at different depths were considered different classes. As shown in Table I, NAPCA with SBE provided the highest target classification (TC) accuracy (i.e., 87.1%) when classifying the target buried at seven different depths and the highest overall classification (OC) accuracy (i.e., 77.0%) when classifying all the ten classes including natural ore and background.

The detailed classification results of the seven target classes are listed in Table II (corresponding to the TC in Table I). The 60 cm DU was difficult to be classified because the spectra were close to those of the natural ore buried 45 cm and 75 cm deep. Interestingly, the four methods applied on the original data (i.e., GC, SBE, SBR, SCR) could provide 100% accuracy for 15 cm DU, while the NAPCA-based methods yielded better results for all the classes. This means the NAPCA-generated feature space is optimal in terms of all the classes but may not for a specific class.

The accuracy for 0.25 s and 0.1 s data were presented in Tables III and IV, respectively. For 0.25 s data, two NAPCA-based methods could provide 90% overall detection accuracy and 70% overall classification accuracy. For 0.1 s data, using NAPCA, the overall detection accuracy could be above 80%; however, the target classification and the overall classification accuracy were only around 60% and 50%, respectively, due to

TABLE II
CLASSIFICATION ACCURACY (%) OF SEVEN TARGET CLASSES

	15cm	23cm	30cm	45cm	60cm	75cm	90cm
GC	100.0	100.0	100.0	95.2	23.8	47.6	95.2
SBE	100.0	77.3	54.5	90.9	50.0	100.0	100.0
SBR	100.0	79.2	79.2	54.2	12.5	87.5	70.8
SCR	100.0	70.8	79.2	83.3	37.5	95.8	75.0
SBE-PCA	83.3	45.8	33.3	91.7	54.2	100.0	100.0
SBR-PCA	91.7	50.0	87.5	20.8	12.5	62.5	16.7
SCR-PCA	87.5	37.5	66.7	54.2	50.0	100.0	58.3
SBE-NAPCA	95.0	95.0	75.0	100.0	50.0	95.0	100.0
SBR-NAPCA	95.2	95.2	76.2	100.0	47.6	95.2	100.0
SCR-NAPCA	90.5	61.9	66.7	95.2	66.7	100.0	90.5

TABLE III
DETECTION AND CLASSIFICATION ACCURACY (%) OF 0.25 S DATA

Methods	TD	NTD	OD	TC	OC
GC	83.3	55.6	75.0	73.8	60.0
SBE	85.7	75.0	82.5	71.4	67.5
SBR	88.1	11.1	65.0	47.6	33.3
SCR	82.1	50.0	72.5	57.1	47.5
SBE-PCA	90.5	83.3	88.3	76.2	66.7
SBR-PCA	78.6	50.0	70.0	45.2	41.7
SCR-PCA	78.6	72.2	76.7	50.0	48.3
SBE-NAPCA	92.9	88.9	91.7	78.6	70.0
SBR-NAPCA	92.9	88.9	91.7	78.6	70.0
SCR-NAPCA	85.7	77.8	83.3	76.2	73.3

TABLE IV
DETECTION AND CLASSIFICATION ACCURACY (%) OF 0.1 S DATA

Methods	TD	NTD	OD	TC	OC
GC	78.6	66.7	75.0	71.4	50.0
SBE	81.0	44.4	70.0	54.8	50.0
SBR	92.9	22.2	71.7	31.0	26.7
SCR	88.1	22.2	68.3	40.5	33.3
SBE-PCA	81.0	50.0	71.7	47.6	45.0
SBR-PCA	71.4	44.4	63.3	35.7	33.3
SCR-PCA	81.0	44.4	70.0	57.1	51.7
SBE-NAPCA	85.7	86.7	86.0	62.9	50.0
SBR-NAPCA	85.7	86.7	86.0	62.9	50.0
SCR-NAPCA	82.9	80.0	82.0	60.0	50.0

low energy counts when sensor dwell time was as short as 0.1 s. In this case, the GC method seemed to be quite stable.

B. Uncertainty Analysis

Tables I–IV show the average accuracy in the 24-fold cross-validations. In order to better describe the accuracy statistics when using different training and test samples, box-plots were generated in Fig. 6 showing the mean and standard deviation for each method (corresponding to Table I). From Fig. 6(a), we can see that GC and SBR-PCA were worse than other six methods; SBE-NAPCA and SBR-NAPCA were the best because the mean accuracy was among the largest and the standard deviation was the smallest. Similarly, in Fig. 6(b)–(e), SBE-NAPCA, SBR-NAPCA, and SCR-NAPCA were better than their counterparts, and ranked among the best methods.

TABLE V
F-TEST FOR THE MEAN ACCURACIES OF THE TEN METHODS

	TD	NTD	OD	TC	OC
F Value	8.8835	13.3817	13.1613	15.2013	22.3821
P Value	<0.0001	<0.0001	<0.0001	<0.0001	<0.0001

TABLE VI
T-TEST FOR THE MEAN ACCURACIES OF THE FOUR GROUPS

		TD	NTD	OD	TC	OC
G_1-G_2	T Value	2.4381	0.0340	1.2705	1.1516	0.7784
	P Value	**0.0187**	0.9730	0.2103	0.2554	0.4403
G_1-G_3	T Value	0.4810	1.3129	1.1242	4.2020	1.3643
	P Value	0.6328	0.1957	0.2668	**0.0001**	0.1791
G_1-G_4	T Value	3.7721	2.6538	4.1059	1.3817	4.2150
	P Value	**0.0005**	**0.0109**	**0.0002**	0.1737	**0.0001**
G_2-G_3	T Value	1.3408	1.3167	0.0167	2.7425	1.7053
	P Value	0.1866	0.1945	0.9868	**0.0087**	0.0949
G_2-G_4	T Value	1.3974	2.7160	2.8236	2.1044	2.4557
	P Value	0.1690	**0.0093**	**0.0070**	**0.0408**	**0.0179**
G_3-G_4	T Value	2.3041	1.3689	2.4237	4.7176	4.0286
	P Value	**0.0258**	0.1777	**0.0194**	**0.0001**	**0.0002**

The ANOVA (analysis of variance) F-test was employed to quantify the statistically significant difference between the mean accuracies of the ten methods (denoted as $\mu_i, i = 1, \ldots, 10$) with the hypothesis test being formulated as

$$H_0 : \mu_1 = \mu_2 = \ldots = \mu_{10}$$
$$H_1 : \text{not all the } \mu_i \text{ are equal.} \quad (15)$$

The results are shown in Table V with significance level being set to be $\alpha = 0.05$ as usual [12]. We can see that all the P values are less than 0.0001, much smaller than $\alpha = 0.05$, indicating that H_0 is rejected. This means there really exist significant differences among the mean accuracies of the ten methods. Based on the F values, Table V also indicates that performance discrepancy is the most obvious for OC and the least obvious for TD, which is the same as illustrated in Fig. 6. Here, error degree of freedom is 230, treatment degree of freedom is 9, and total degree of freedom is 239.

T-test was also used to analyze the significance of performance discrepancy between different groups: group1 (G_1):

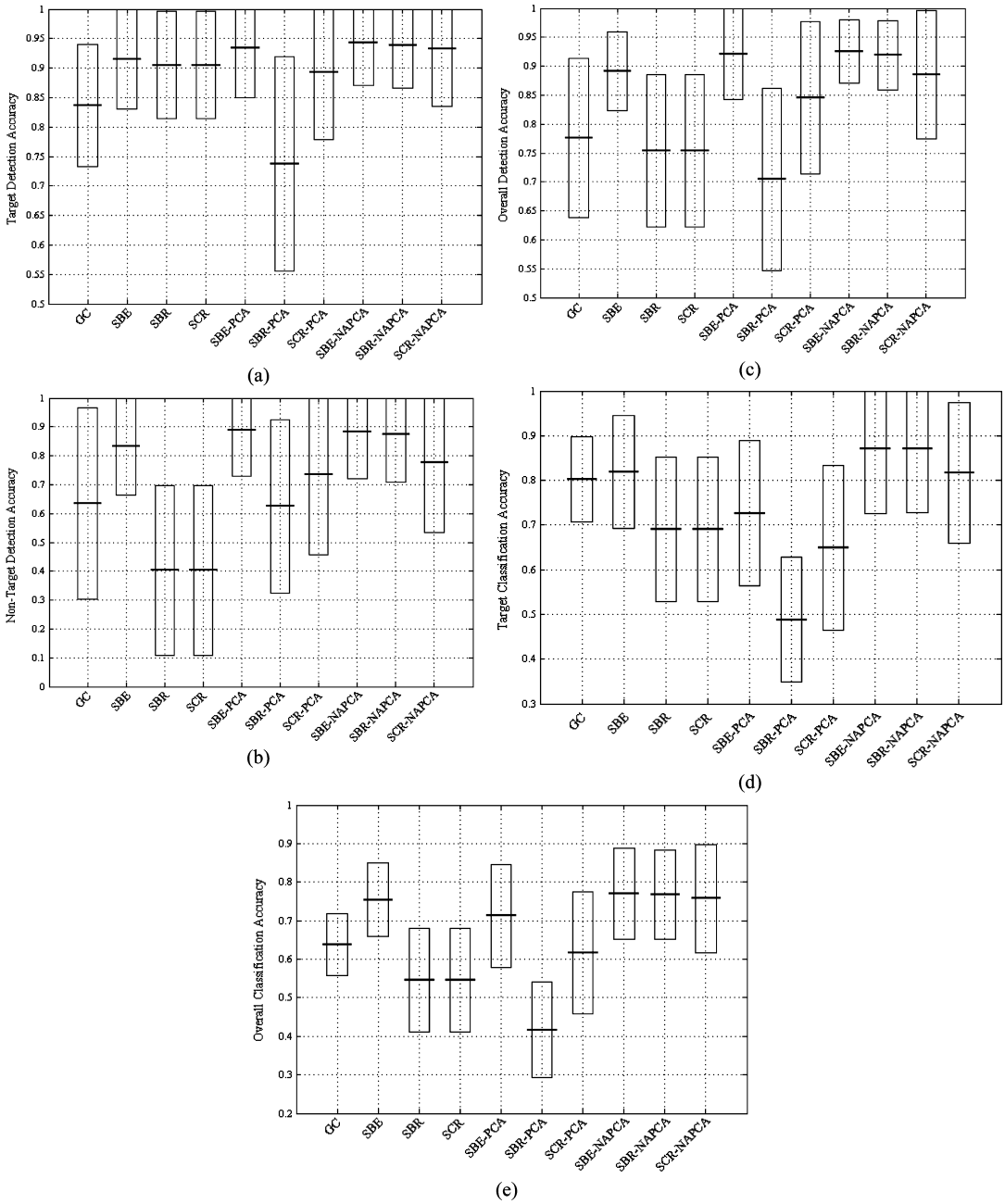

Fig. 6. Boxplots for 24-fold cross-validation using the entire dataset. (a) Target Detection (TD) Accuracy, (b) Non-target Detection (NTD) Accuracy, (c) Overall Detection (OD) Accuracy, (d) Classification Accuracy of Seven Target Classes (TC), (e) Overall Classification Accuracy of Ten Classes (TC).

{GC}; group2 (G_2): {SBE, SBR, SCR}, group3 (G_3): {SBE-PCA, SBR- PCA, SCR-PCA}, group4 (G_4): {SBE-NAPCA, SBR-NAPCA, SCR-NAPCA}. The $\mathrm{G}_i - \mathrm{G}_j$ test is formulated as

$$H_0 : m_i = m_j$$
$$H_1 : m_i \neq m_j \tag{16}$$

where m_i is the mean accuracy of G_i, for $i = 1, 2, 3, 4$. The significance level being set to be $\alpha = 0.05$ as usual. Small samples inferences for two samples are considered. The degree of freedom equals the number of samples in the two groups minus 2. If the P value is smaller than $\alpha = 0.05$, H_0 is rejected which means there exists material difference between the performance of the two groups under test. The T-test results were shown in Table VI where the P values less than $\alpha = 0.05$ were highlighted. As we can see, in all the tests related to the NAPCA group G_4, the significance was very obvious. For instance, the test between G_2 and G_4 showed that all the accuracies except TD demonstrated great improvement, which means applying NAPCA was better than the original transforms; the test between G_3 and G_4 also showed great improvement except NTD, which means NAPCA was a better choice than PCA.

C. Experiment Using Data Containing Difficult Classes Only

This experiment was conducted when the three easy classes: DU buried 15 cm, 23 cm, and 30 cm deep, were removed.

TABLE VII
DETECTION AND CLASSIFICATION ACCURACY (%) OF DIFFERENT METHODS FOR THE DATASET CONTAINING SEVEN DIFFICULT CLASSES

Methods	TD	NTD	OD	TC	OC
GC	75.0	66.7	71.4	69.8	51.2
SBE	85.9	84.1	85.1	85.9	72.8
SBR	83.3	41.7	65.5	63.5	45.8
SCR	81.3	72.2	77.4	72.9	66.1
SBE-PCA	87.5	81.9	85.1	85.4	73.2
SBR-PCA	56.3	63.9	59.5	22.9	23.2
SCR-PCA	83.3	77.8	81.0	64.6	61.9
SBE-NAPCA	89.1	84.1	87.0	87.0	73.9
SBR-NAPCA	86.5	83.3	85.1	84.4	71.4
SCR-NAPCA	85.4	80.6	83.3	83.3	67.9

Table VII lists the average detection accuracy of cross-validation, where NAPCA could improve the performance of SBE, SBR, and SCR while PCA did not necessarily bring about improvement. Table VII also lists the average classification accuracy for the seven classes (with four target classes), where NAPCA-based methods were among the best.

V. CONCLUSION

In this paper, we propose an approach for buried radioactive target detection and classification, which applies spectral transformation followed by PCA or NAPCA. To meet the requirement of practical survey mapping, we focus on the circumstance when sensor dwell time is very short (i.e., less than 1 s). In this case, the gamma spectroscopy collected by an NaI detector can be sparse, random, and dominated by energy counts from the background. We believe an appropriate spectral transform can alleviate the effects from spectral noisy variation and background clutters, while NAPCA, a better choice than PCA, can extract major features for the following detection and classification. Thus, it can generally improve the target detection and classification performance after a certain spectral transform is applied.

For SBR and SCR, a known background measurement is needed. For real field data, background may be changed with geolocation. Under such circumstance, SBR and SCR should be applied locally by using a local background measurement. Even for the data collected at the same location (e.g., the lab data), the background measurement is changed with time due to counting uncertainty when sensor dwell time is very short. This is why a background measurement normalized by another background measurement using SBR or SCR is not a constant 1 or 0. Such variation shows the importance of employing a statistical approach (e.g., PCA and NAPCA) instead of the traditional deterministic approach. It also motivates us to employ a multi-dimensional technique, where all the energy channels/bins are explored simultaneously for decision-making rather than a single or a few channels only.

It is worth mentioning that the performance of all the three spectral transforms is varied with the bin-width selection. How to automatically select an optimal bin-width for each transform is under investigation. However, using the NAPCA-transformed data, these three spectral transforms generally can provide better detection and classification than other methods, such as GC, applied on the original data.

ACKNOWLEDGMENT

The authors would like to thank C. Waggoner and D. Rogers in the Institute for Clean Energy Technology at Mississippi State University for providing the lab data.

REFERENCES

[1] D. C. Stromswold, J. Darkoch, J. H. Ely, R. R. Hansen, R. T. Kouzes, B. D. Milbrath, R. C. Runkle, W. A. Sliger, J. E. Smart, D. L. Stephens, L. C. Todd, and M. L. Woodring, "Field tests of a NaI(Tl)-based vehicle portal monitor at border crossings," in *IEEE Nuclear Science Symp. Conf. Record*, 2004, vol. 1, pp. 196–200.

[2] R. T. Kouzes and J. H. Ely, "The role of spectroscopy versus detection for border security," *J. Radioanalyt. Nucl. Chem.*, vol. 276, no. 3, pp. 719–723, 2007.

[3] D. S. Haslip, T. Cousins, D. Estan, and T. Jones, "Field detection of depleted uranium final report of tasking W28476KR00Z (DSSPM)," Defence Research Establishment, Ottawa, (Ontario), Report No: DREO TM-2000-049, 2000.

[4] K. K. Anderson, K. D. Jarman, M. L. Mann, D. M. Pfund, and R. C. Runkle, "Discriminating nuclear threats from benign sources in gamma-ray spectra using a spectral comparison ratio method," *J. Radioanalyt. Nucl. Chem.*, vol. 276, pp. 713–718, 2008.

[5] D. M. Pfund, R. C. Runkle, K. K. Anderson, and K. D. Jarman, "Examination of count-starved gamma spectra using the method of spectral comparison ratios," *IEEE Trans. Nucl. Sci.*, vol. 54, no. 4, pp. 1232–1238, Aug. 2007.

[6] J. H. Ely, R. T. Kouzes, J. E. Schweppe, E. R. Siciliano, D. M. Strachan, and D. R. Weier, "The use of energy windowing to discriminate SNM from NORM in radiation portal monitors," *Nucl. Instrum. Methods Phys. Res.*, vol. 560, no. 2, pp. 373–387, 2006.

[7] R. C. Runkle, M. F. Tardiff, K. K. Anderson, D. K. Carlson, and L. E. Smith, "Analysis of spectroscopic radiation portal monitor data using principal components analysis," *IEEE Trans. Nucl. Sci.*, vol. 53, no. 3, pp. 1418–1423, June 2006.

[8] T. M. Cover and P. E. Hart, "Nearest neighbor pattern classification," *IEEE Trans. Inf. Theory*, vol. 13, pp. 21–27, 1967.

[9] A. A. Green, M. Berman, P. Switzer, and M. D. Craig, "A transformation for ordering multispectral data in terms of image quality with implications for noise removal," *IEEE Trans. Geosci. Remote Sensi.*, vol. 26, pp. 65–74, 1988.

[10] J. B. Lee, A. S. Woodyatt, and M. Berman, "Enhancement of high spectral resolution remote sensing data by a noise-adjusted principal components transform," *IEEE Trans. Geosci. Remote Sensi.*, vol. 28, pp. 295–304, 1990.

[11] R. E. Roger and J. F. Arnold, "Reliably estimating the noise in AVIRIS hyperspectral imagers," *Int. J. Remote Sensi.*, vol. 17, pp. 1951–1962, 1996.

[12] A. C. Tamhane and D. D. Dunlop, *Statistics and Data Analysis: From Elementary to Intermediate*. Engelwood Cliffs, NJ: Prentice Hall, 2000.